A New Paradigm for Distributed Generation Management Considering the Renewable Energy Uncertainties and Demand Response Resources

Peyman Ghanbari-Mobarakeh*, Mohammadreza Moradian*,**‡

* Department of Electrical Engineering, Najafabad Branch, Islamic Azad University, Najafabad, Iran.

** Smart Microgrid Research Center, Najafabad Branch, Islamic Azad University, Najafabad, Iran.

(p.ghanbari@iaun.ac.ir, moradian@iaun.ac.ir)

‡ Mohammadreza Moradian; Corresponding Author, Assistant Professor, Department of Electrical Engineering, Najafabad Branch, Islamic Azad University, Iran, Tel: +983142292623, Fax: +983142291016, moradian@iaun.ac.ir

Received: 22.12.2018 Accepted: 19.01.2019

Abstract- In recent decades, the prevalence of microgrids with the resolution of more exploitation of demand-side renewable energy resources has been vastly increased. The advantages of microgrids such as reduction of operation costs, use of clean renewable energy, and improvement in the reliability of the system have assumed significant attention to this subject. In this regard, the optimization of microgrids is an important item, which reinforces the plus sides of microgrid scheme. The demand response programs (DRPs) are practical tools accessible for the operator to facilitate and optimize the management of the grid's operation and are counted as novel evolutions in modern power systems. Demand response implies that the consumers can have participation in reshaping and correction of the load pattern. These programs can achieve considerable profits from both consumers and the grid point of view such as reduction of load shedding, mitigation of generation cost, smoothing the load curve, alleviation of price fluctuations in electricity markets etc. In this study, a new energy management scheme is proposed in order to obtain the optimized performance of the microgrid in presence of renewable resources. The short-term operational costs are declined by incorporation of incentive-based programs (IBP). The results of the simulations are illustrated through three scenarios to assess the improvements in costs and emissions. The implication of the presence of renewable and demand response resources is investigated in these scenarios. Moreover, the Chicken swarm optimization algorithm is employed to conduct the optimization of the objective function. The results reveal that the suggested scheme is effective and beneficial.

Keywords: Microgrid, uncertainty, energy management system, renewable energy resources, demand response resources.

1. Introduction

The dramatic increase in energy consumption and massive emission of greenhouse gases due to energy consumption have aroused serious mounting concern, which has been leading to one of the most vital issues of the modern world in the 21st century. Hence, feasible solutions must be put forward in order to deal with the problems. Some currently used solutions are the efficiency improvement in the industries and energy audit, reduction of residential and commercial losses, and correction and upgrade of energy management principles. Recent studies have implied that around 20% to 30% of the consumption can be mitigated without any physical change in the system's structure only with the employment of optimized and managed performances and decisions. Therefore, some options are declared by the researchers to tackle this problem, one of which is to utilize distributed generation resources, particularly renewable resources such as wind and solar, to alleviate the emission and losses. Hence, microgrid schemes are introduced as a new concept in the modern power system operation and planning, which are mostly based on renewable resources along with smart grid infrastructure, and they are usually capable of exchanging power with the main grid or other microgrids [1]. The generation resources include solar panel, fuel cell, wind turbines, battery, micro-turbine, and

diesel generator. Besides, if the microgrids can be able to exchange power with the upstream grid, they operate more efficient economically and technically. The presence of controllable loads for consumption pattern modification is another advantage of microgrids. The implementation of demand response programs (DRPs) has become viable thanks to information and telecommunications infrastructures and advanced metering devices [2].

So far, various researches are conducted on the deployment of distributed generation. In [3], the size of an isolated microgrid, which is exclusively supplied by renewable energy resources, is optimized. In the supposed microgrid, an energy storage facility is utilized to improve the reliability of microgrid. In [4], various approaches are compared in order to obtain the most optimum size of microgrids, which highly depend on renewable resources. Besides, the optimization of the size of a microgrid's components including photovoltaic, wind, and battery bank is carried out using an iterative approach in [5]. The aforementioned multi-objective optimization problem is subject to maximize the reliability of power supply in addition to the minimization of normalized electricity price. The mentioned study is conducted regardless of DRPs and elasticity of demand as well as the stochastic nature of renewable resources and the loads. DRPs are mainly able to decrease the operational costs of power systems. In these programs, the consumers are promoted or forced to change their load pattern corresponded with the change in the time-based electricity tariffs or they are encouraged to decrease their consumption or shift them to receive financial incentives, especially at peak hours when the market prices are high and the reliability and security of the system is threatened [6]. The authors in [7] have proposed a model, in which the microgrid's operator does not impose any obligation on the consumers, and the customers do not receive any incentive for participation in the program. In [8], the power dispatch management is studied exclusively for an isolated system. In [9], the impact of responsive loads on generation management of an isolated microgrid is investigated. In [10], a cost assessment is carried out for a microgrid in two cases of capable of selling electricity to the upstream network or incapable of exchanging power with the main grid. In this work, the responsive load is considered to be the maximum rate of interruptible loads. In addition, in a comprehensive work [11], the microgrid is considered to be disconnected from the main grid and the implication of uncertainty of renewable resources as well as environmental concepts and electricity production management are taken into account. In [12], similar to the [10], the cost-effective assessment is conducted for a microgrid, which is isolated from the upstream grid. In this work, various scenarios are defined, in which different configuration of generation resources and energy storage devices are compared. Moreover, in the reference [13], a day-ahead schedule and a real-time schedule in five-minute intervals are introduced. In [14], a study is conducted about bi-level cost management for microgrids. In the first stage, the aim is to maximize the profit of the system and in the second stage, the optimization is done subject to minimize the reserve costs regard to redressing the forecasting errors.

The renewable energy resources such as wind, solar as well as the scheduled load have inherent stochastic nature. In the literature, described above, the energy management, the operation of a microgrid, and optimization of the microgrids' components are evaluated regardless of the intermittent nature of these parameters. Although the neglect of stochastic nature eases the problem-solving procedure and simplifies the modeling, this matter has a negative impact on the reliability and social welfare indices. In the following part, some studies have been stated, in which the stochastic nature of the resources and loads are taken into consideration. In [15], two probabilistic density functions for the forecast of wind speed and solar radiation have been employed to perform the stochastic operation scheduling of the microgrid. In [16], the impact of uncertainty on the determination of the size of components of an off-grid microgrid including photovoltaic and battery is analyzed. In this paper, the daily electrical load is modeled probabilistically, and it is optimized based on the net present cost and loss of load probability. In the previous works, the impacts of demand response resources on the optimization of the size of microgrid's components are not explored.

In this paper, presented by us, a model of generation dispatch aiming to minimize the operational costs and emission of greenhouse gases regard to the use of incentive-based DRPs is proposed. The consumers are classified into three categories of residential, commercial and industrial, which can have voluntary participation in DRPs. The Chicken swarm optimization algorithm (CSO) is employed as the vehicle of optimization subject to minimize the operational costs and emission. In section 2, the system's components are individually explained and their corresponding uncertainties are modeled. In section three, the objective function and the prevailing constraints of the problem are described. In the fourth section, the CSO algorithm is thoroughly explained. In section five, the simulation results are presented and discussed. Ultimately, in the last section, the conclusions are drawn.

2. The Modeling of the System's Components

The modeling of inherent uncertainties and forecasting errors are of the most important items in the design of microgrids. In this study, the applied uncertainties are renewable energy resources (photovoltaic modules and wind turbines), the targeted hourly load level and the hourly electricity price. The historical records of the uncertain parameters are provided to obtain an appropriate probability density function. Besides, at the end of this section, the modeling of the energy storage facility is also described **[17].**

2.1. Renewable Energy Resource Modeling

The amount of solar power generation corresponds with the solar irradiance and the ambient temperature. In addition, wind power generation depends on wind speed and the type of the utilized turbine. These characteristics of a turbine rely on the geographic features of the installation site. Therefore, initially, the solar radiation, temperature and wind speed historical data of the location of installation site of the turbine must be provided and analyzed [18].

a. Solar Irradiance Modeling

The output power of each photovoltaic (PV) array can be specified by Eq. (1):

$$P_{pv} = P_{STC} \times \frac{S}{S_{STC}} \times \left[1 + k_{MPT}\left(T_c - T_a\right)\right] \quad (1)$$

P_{STC} represents the active power of PV module in the standard test condition, S_{STC} is the radiation intensity in the standard test condition, T_c shows the PV cell temperature, k_{MPT} denotes the heat factor of maximum power, and S and T_a stand for radiation intensity and temperature of the installation site respectively [19]. Beta distribution employed for modeling of the radiation intensity of S (kW/m^2) at the time interval of t, which can be described by Eq. (2):

$$\begin{cases} f_s(s) = \dfrac{\Gamma(\alpha+\beta)}{\Gamma(\alpha)\Gamma(\beta)} \times (s)^{\alpha-1} \times (1-s)^{\beta-1} \\ \beta = (1-\mu_s) \times \left(\dfrac{\mu_s(1+\mu_s)}{(\sigma_s)^2} - 1 \right) \quad ; \quad \alpha = \dfrac{\mu_s \times \beta}{(1-\mu_s)} \end{cases} \quad (2)$$

Where, Γ stands for Gamma function, and α and β represents can be obtained by the above equation, in which μ_s represents the mean value and σ_s is the standard deviation.

b. Wind Modeling

The Weibull distribution function can be used appropriately to model the wind generation [20]. This function is formulated using three parameters as shown in Eq. (3):

$$\begin{cases} f_w(v) = \dfrac{k}{c}\left(\dfrac{v-v_0}{c}\right)^{k-1} \times \exp\left[-\left(\dfrac{v-v_0}{c}\right)^{k}\right] \\ k = \left(\dfrac{\sigma_v}{\mu_v}\right)^{-1.086} \quad ; \quad c = \dfrac{\mu_v}{\Gamma(1+\dfrac{1}{k})} \end{cases} \quad (3)$$

In the above equation, $f_w(v)$ represents the Weibull distribution function, v_0 stands for location parameter, k denotes the shape parameter, and c shows the scale parameter in Weibull distribution. In above, μ_v and σ_v are the mean value and standard deviation of wind speed respectively [21]. Eq. (4) shows the correlation between wind speed and output active power of wind turbines.

$$P_w = \begin{cases} 0 & v \le v_{ci} \\ k_1 v + k_2 & v_{ci} \le v \le v_r \\ P_r & v_r \le v \le v_{co} \\ 0 & v \ge v_{co} \end{cases} \quad (4)$$

v_r is the rated wind speed, v_{ci} shows the cut-in speed characteristic of the wind turbine, and v_{co} represents the cut-out speed characteristic of the turbine. P_r indicates the rated power of the wind turbine. In addition, k_1 and k_2 are randomly sampled numbers derived from [0,1] based on chosen distribution function [22].

$$k_1 = \frac{P_r}{v_r - v_{ci}} \; ; \; k_2 = -k_1 \times v_{ci} \quad (5)$$

2.2. Energy Price and Demand

The intermittent and volatile nature of the demand and the hourly electricity price can be modeled by a normal distribution as employed in Eq. (6). As mentioned before, μ represents the mean value and σ denotes the standard deviation, and x shows can be active or reactive power of demand [23].

$$f_N(x) = \frac{1}{\sqrt{2\pi\sigma}} \exp\left[\frac{(x-\mu)^2}{2\sigma^2}\right] \quad (6)$$

2.3. Micro-turbine Model

The micro-turbine (MT) technology is an advanced model of gas turbines, which is manufactured in smaller scales and operates at higher rotational speeds of turbine blades. This technology has some advantages over gas turbines such as low noise pollution and more flexibility in consuming fuel. They are usually manufactured in the range of 25 to 200 kW and their speed varies from 5000 to 90000 rpm [24]. The output voltage is about 400 v and the bearings are of air type. The MT cost function can be characterized by Eq. (7):

$$F_{t,MT} = C_{MT} \times F_{MT} \times P_{t,MT} \times \Delta T + OM_{t,MT} \quad (7)$$

In the above equation, $F_{t,MT}$ represents the total operational cost of the turbine ($), C_{MT} is the fuel cost coefficient of the MT ($/m^3) that is considered to be 0.3571 $/m^3 for the natural gas, F_{MT} shows the amount of consumed fuel for generation of one kWh electrical energy (m^3/kWh), which is assumed to be 0.85 m^3/kWh in this study. $P_{t,MT}$ denotes the output power of the MT and is regarded as one of the decision-making variables (kW). Besides, Δt is the scheduling interval which is supposed to be equal with 1 hour in this work. $OM_{t,MT}$ expresses the O&M costs ($), which is corresponded with the amount of generated power at each hour [25].

$$OM_{t,MT} = k_{OC} \times P_{t,MT} \times \Delta T = 0.00587 \times P_{t,MT} \times \Delta T \quad (8)$$

In the above equation, the proportional constant of k_{OC} is supposed to be 0.00587 $/kWh. The output power of the MT is also restrained by the following boundaries:

$$P_{MT}^{min} \le P_{t,MT} \le P_{MT}^{max} \quad (9)$$

2.4. Energy Storage System

The storage units can have three main applications of bulk energy time-shifting, frequency stability regulation (in small scale), and power reliability [26, 27]. The appropriate type of storage must be selected according to their application (charge and discharge speed, quantity of charge-discharge cycles, and scalability) [28-31]. The charging and discharging rates are important factors in energy storage systems. Thus, Eq. (10) is used in order to model this restriction [32-34].

$$\begin{cases} W_{ess}^{t} = W_{ess}^{t-1} + \eta_{charge} P_{charge} \Delta t - \dfrac{1}{\eta_{discharge}} P_{discharge} \Delta t \\ W_{ess,\min} \le W_{ess}^{t} \le W_{ess,\max} \\ P_{charge,t} \le P_{charge,\max} \; ; \; P_{discharge,t} \le P_{discharge,\max} \end{cases} \quad (10)$$

Where, $W_{ess,min}$ is the minimum storable level of energy in the ESS, $W_{ess,max}$ shows the maximum level of energy that can be stored in ESS, and $P_{ch/dis,max}$ represents the maximum nominal charging/discharging rate of the ESS within the interval of Δt. Each storage facility, such as a battery, can be charged or discharged with a specific rate, and the accessible amount of power which can be supplied by a storage device is limited to this rate. The storage utility normally stores electricity at off-peak and deliver it to the microgrid at peak.

3. Problem Outlines

3.1. Demand Response Model

The microgrid's scheme is designed so that the wind and solar units are used mainly to meet the demand basically, and the stochastic deficiency must be redressed by demand response resources. The demand would be supplied by MT, wind, solar, battery, and demand response resources (as virtual demand-side power plants) with the target 24-hour period. The purpose of this study is to minimize the operational costs and emissions and to compare the cases of inclusion and exclusion of demand response resources, while the prevailing equality and inequality constraints are imposed with respect to the uncertainties of wind and solar generation. In this study, the consumers are classified into three types of residential, commercial, and industrial, and the following equations demonstrate the model of these loads [35].

$$RP(r,t) = RC(r,t) \times \pi_{r,t} \qquad RC(r,t) \le RC_t^{\max} \tag{11}$$

$$CP(c,t) = CC(c,t) \times \pi_{c,t} \qquad CC(c,t) \le CC_t^{\max} \tag{12}$$

$$IP(i,t) = IC(i,t) \times \pi_{i,t} \qquad IC(i,t) \le IC_t^{\max} \tag{13}$$

In the above-stated formulas, r, c and i stand for residential, commercial and industrial consumers respectively. $RC(r,t)$, $CC(c,t)$, and $IC(i,t)$ represent the amount of consumption reduction by each type of the loads at the interval of t. RC_t^{max}, CC_t^{max}, and IC_t^{max} are the maximum offered consumption reduction by each type of loads. In addition, $\pi_{r,t}$, $\pi_{c,t}$ and $\pi_{i,t}$ represent the incentive for each type of demand at interval of t; and $RP(r,t)$, $CP(c,t)$ and $IP(i,t)$ show the cost of demand response by the residential, commercial and industrial loads at the interval of t.

3.2. Objective Function

The objective function of this study includes minimization of operational costs of the microgrid and emission of greenhouse gases, in regard or disregard to the influence of demand response resources.

a. Operational objective function

The operational objective function consists of cost functions for each generation unit in addition to their specific startup and shutdown costs added by the cost of the energy storage unit and the cost of implementation of DRPs for the entire time horizon. These constraints are described as the following equations:

$$\min \quad f_1(x) = \sum_{t=1}^{T} \begin{pmatrix} \cos t_{DG}(t) + ST_{DG}(t) + \\ \cos t_s(t) + \cos t_{Grid}(t) + \cos t_{DR}(t) \end{pmatrix} \tag{14}$$

$$\cos t_{DG}(t) = \sum_{i=1}^{Ng} u_i(t) P_{DGi}(t) B_{DGi}(t) \tag{15}$$

$$ST_{DG}(t) = \sum_{i=1}^{Ng} S_{DGi} \left| u_i(t) - u_i(t-1) \right| \tag{16}$$

$$\cos t_s(\mathrm{t}) = \sum_{j=1}^{Ng} \left[u_j(t) P_{sj}(t) + S_{sj}(t) \left| u_j(t) - u_j(t-1) \right| \right] \tag{17}$$

$$\cos t_{Grid}(t) = \begin{pmatrix} u_{buy}(t) P_{Grid-Buy}(t) B_{Grid-Buy}(t) \\ -u_{sell}(t) P_{Grid-sell}(t) B_{Grid-sell}(t) \end{pmatrix} \tag{18}$$

$$\cos t_{DR}(t) = P_{DR}(t) B_{DR}(t) \tag{19}$$

$$P_{DR}(t) = \sum_r RC(r,t) + \sum_c CC(\mathrm{c},t) + \sum_i IC(i,t) \tag{20}$$

In above, $P_{DGi}(t)$ and $P_{sj}(t)$ are the output power of the i^{th} generator and the j^{th} storage unit at interval t. Besides, $B_{DGi}(t)$ and $B_{sj}(t)$ are the offers of the i^{th} generator and the j^{th} storage unit at interval t. $S_{DGi}(t)$ and $S_{sj}(t)$ are defined to show the startup and shutdown costs of the i^{th} generator and the j^{th} storage unit at the interval of t. In addition, $P_{Grid\text{-}buy}(t)$ and $P_{Grid\text{-}sell}(t)$ are the bought or sold power from/to the upstream distribution company at the interval of t. furthermore, $B_{Grid\text{-}buy}(t)$ and $B_{Grid\text{-}sell}(t)$ are the bids of the consumers to exchange power with the main grid at the t^{th} period. Ultimately, $P_{DR}(t)$ and $B_{DR}(t)$ are the amounts of power and the suggested price for the participants of the DRP [36].

When the objective function is called, x is considered as the decision making variable, which composed of the output power of each individual generation unit, the amount of power exchange with the upstream grid, the amount of load reduction (load shedding) provided by the DR participants, and the ON/OFF state of the units for the targeted prospect of the dispatch schedule for the next day, which can be displayed as below:

$$\begin{cases} x = \left[P_g, U_g \right]_{1 \times 2nT} \\ P_g = \left[P_{DG1}, P_{DG2}, ..., P_{DGN_{DG}}, P_{s1}, P_{s2}, ..., P_{sN_s}, P_{Grid}, P_{DR} \right] \\ U_g = \left[U_{DG1}, U_{DG2}, ..., U_{DGN_{DG}}, U_{s1}, U_{s2}, ..., U_{sN_s}, U_{Grid}, U_{DR} \right] \\ n = N_{DG} + N_s + 2 \end{cases} \tag{21}$$

Where n represents the number of decision-making variables; N_{DG} and N_s are the sets of generation and storage units; T denotes the time horizon of the schedule, and P_g signifies the active power vector, which consists of all DG and storage units as well as participants of demand response resources. U_g demonstrates the state vector of the units and it indicates which unit is ON or OFF during the target time horizon.

b. Greenhouse gases objective function

The emission objective function is considered to be composed of CO_2 (carbon dioxide), SO_2 (sulfur dioxide), NO_x (Nitrogen dioxide).

$$\begin{aligned} \min \quad & f_2(x) \Rightarrow \min \sum_{t=1}^{T} Emission(t) \\ & = \sum_{t=1}^{T} \begin{Bmatrix} emission_{DG}(t) + \\ emission_s(t) + emission_{Grid}(t) \end{Bmatrix} \\ & = \min \sum_{t=1}^{T} \begin{Bmatrix} \sum_{i=1}^{Ng} \left[u_i(t) P_{DG_i}(t) E_{DG_i}(t) \right] \\ + \sum_{j=1}^{Ns} \left[u_j(t) P_{s_j}(t) E_{s_j}(t) \right] + P_{Grid}(t) E_{Grid}(t) \end{Bmatrix} \end{aligned} \tag{22}$$

In the above equation, $E_{DGi}(t)$, $E_{sj}(t)$, and $E_{Grid}(t)$ represent the amount of emission in kg/MWh^{-1} for each generator, storage devices, and grid-side provided power at the interval of t. The proposed objective function is comprised of the operation cost and the emission cost of existing generating units in the microgrid that is shown by Eq. (23) and must be minimized.

$$f = \min \sum_{t=1}^{24} \{f_1 + f_2\} \tag{23}$$

3.3. Problem Constraints

These constraints include load equality, the active generation limitation, and battery restriction which can be pointed out by the following equation:

$$\sum_{i=1}^{Ng} P_{DG_i}(t) + \sum_{j=1}^{Ns} P_{s_j}(t) + u_{buy}(t) P_{Grid-Buy}(t) = \sum_{L=1}^{N_L} P_{DemandL}(t) + u_{sell}(t) P_{Grid-sell}(t) - P_{DR}(t) \tag{24}$$

Where $P_{demandL}(t)$ indicates the demand level of L, and N_L is the total number of demand's levels.

$$\begin{cases} P_{DGi,\min}(t) \le P_{DGi}(t) \le P_{DGi,\max}(t) \\ P_{sj,\min}(t) \le P_{sj}(t) \le P_{sj,\max}(t) \\ P_{Grid,\min}(t) \le P_{Grid}(t) \le P_{Grid,\max}(t) \end{cases} \tag{25}$$

In above, $P_{DGi,min}(t)$, $P_{sj,min}(t)$, and $P_{Grid\ min}(t)$ are the minimum capability of providers (the i^{th} DG, j^{th} storage unit, or upstream distribution grid) to maintain demanded power. $P_{DGi,max}(t)$, $P_{sj,max}(t)$, and $P_{Grid\ max}(t)$ represent the maximum generation capability of each supplier at the interval of t.

$$\begin{aligned} &\psi_j(t) = \psi_j(t-1) - \frac{1}{\lambda_{Dj}} u_{Dj}(t) P_{Dsj}(t) + \lambda_{cj}(t) u_{cj}(t) P_{Csj}(t) \\ &u_{Dj}(t) + u_{cj}(t) \le 1 \\ &\psi_{\min}(t) \le \psi_j(t) \le \psi_{\max}(t) \\ &\psi_j(t) = \psi_e \end{aligned} \tag{26}$$

Where, the first equation indicates the battery capacity, which can vary hour to hour and relies on charging and discharging rates. The second equation points out that the battery can be charged or discharged at each individual hour but not simultaneously. $\Psi_j(t)$ and $\Psi_j(t\text{-}1)$ express the stored energy at the current and previous hour. Besides, $P_{Csj}(t)$ and $P_{Dsi}(t)$ are the allowed charge/discharge rate of the storage. λ_{Dj} and λ_{Cj} are the round-trip efficiency of the conversion loop in discharging and charging modes.

4. The Chicken Swarm Optimization Algorithm

Chicken swarm optimization is a stochastic optimization approach that is inspired by the searching behavior of the swarm of chickens. For simplicity of chickens' behaviors, the following rules are idealized [37]:

1- The chicken swarm consists of several groups. Each group includes a dominant rooster, some hens, and chicks.

2- The way of division of chicken swarm into several groups and the identification of chickens (including roosters, hens, and chicks) all relies on chicken' fitness value. The chickens that acquired the better fitness values are would be treated as roosters so that each one the roosters are dedicated head of one group. The chickens that have obtained the worst fitness values are acted as chicks and the rest of the chickens are would be designated as hens. The hens are dispersed in the groups randomly. Besides, the mother-child relationship would be established by random sampling (between chicks and hens).

3- The parameters of the mother-child relationship, dominance relationship, and hierarchal order in a group will not change and will remain fixed. The status of each parameter will be updated every G iteration.

4- The hens follow the head of the group which is a rooster to look for food. The chicks usually search for food in the vicinity of their mother. The chickens inherently prevent each other from eating their own food. It is assumed that the chickens steal the ones good food which is found by other chickens. The superior chickens are more probable to win the competition to find food. In another word, they dominant chickens have the advantage to be survived.

The parameters of *RN*, *HN*, *CN*, and *MN* stand for the quantity of the roosters, the number of hens, the number of chicks, and the number of mother hens, respectively. It is ruled that better *RN* chickens are selected as roosters, while worse *CN* chickens are treated as chicks. The rest of the chickens will be regarded as hens. Each individual (roosters, hens, and chicks) will be described by their position of $X^t_{i,j}(i\epsilon[1,...,N], j\epsilon[1,...,N])$ at the time step of t, and they will look for food within a D-dimensional space. In this study, the minimal values are more desired, and the roosters (*RN* chickens) will correspond to the individuals which have minimal fitness values. The position updating function of each individual defers from other ones. These updating functions will be explained in the following part [38]:

A. The movement of the roosters

If a rooster has better fitness value (more minimal) it will have priority over the other roosters with worse fitness values to access food. In order to simplify the approach, this situation can be simulated by the assumption that the rooster with more optimal fitness values can search a wider range of places for food. These phenomena can be formulated as follows:

$$x^{t+1}_{i,j} = x^t_{i,j} * (1 + Randn(0, \sigma^2)) \tag{27}$$

$$\sigma^2 = \begin{cases} 1 & ,if \ \ f_i \le f_k, \\ \exp\left(\frac{(f_k - f_i)}{|f_i| + \varepsilon}\right) & ,otherwise, \end{cases} \quad k \in [1, N], k \ne i \tag{28}$$

Where, $Randn(0,\sigma^2)$ denotes the normal distribution with the mean value of 0 and the standard deviation of σ^2. The parameter of ε (which is the smallest constant value in a computer) is assigned to avoid the error of division by zero. k indicates the index of the rooster, which is chosen by random sampling from the set of roosters. f shows the fitness value of the corresponding x.

B. The hens' movement

The hens follow their own leader rooster of the group to forage for the foods. In addition, they can find the foods of other individuals by chance. However, they may be repressed by other chickens. The more dominant hens certainly have the advantage in competing for gaining food than the more submissive hens. These matters can be modeled mathematically as below:

$$x^{t+1}_{i,j} = \begin{pmatrix} x^t_{i,j} + S_1 * Rand * (x^t_{r1,j} - x^t_{i,j}) \\ + S_2 * Rand * (x^t_{r2,j} - x^t_{i,j}) \end{pmatrix} \tag{29}$$

$$S_1 = \exp((f_i - f_{r1}) / (abs(f_i) + \varepsilon)) \tag{30}$$

$$S_2 = \exp((f_{r2} - f_i)) \tag{31}$$

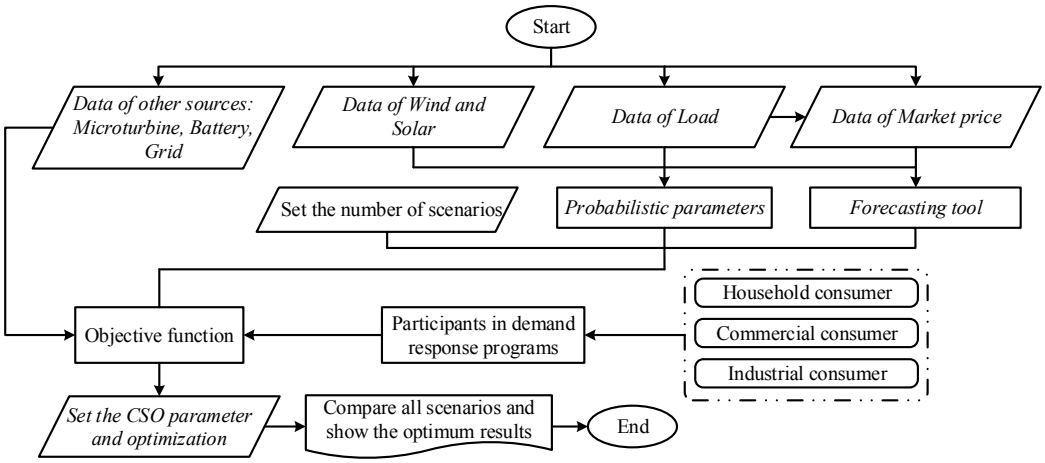

Fig. 1. The flowchart of the optimized scheduling of the targeted microgrid

Where *Rand* is a randomly sampled number derived from the uniform distribution. Besides, $r1\epsilon[1,...,N]$ represent the index of the rooster, which is a group-mate of the i^{th} hens, while $r2\epsilon[1,...,N]$ stands for the index of a chicken (rooster or hen), which has been randomly chosen from the swarm. It can be easily perceived that $r_1 \neq r_2$.

C. The chicks' movement

The chicks follow their mothers to find food that can be modeled by Eq. (32).

$$x_{i,j}^{t+1} = x_{i,j}^{t} + FL * (x_{m,j}^{t} - x_{i,j}^{t}) \quad (32)$$

In the above equation, $x_{m,j}{}^{t}$ defined the position of the i^{th} mother ($m\epsilon[1,N]$). $FL(FL\epsilon(0,2))$ signifies the fact that the chicks would follow their own mother to forage for food. Paying attention to the individual differences, the FL of each chick must be chosen between 0 and 2.

$$f_{\theta} = \omega \times E + (1-\omega)\frac{\sum_i \theta_i}{N} \quad (33)$$

The role of CSO in the procedure of the optimization problem is illustrated in Fig. 1. Fig. 2 shows the semi-code of CSO algorithm.

```
Initialize RN, HN, CN, MN, G;
Randomly initialize each chicken in the swarm Xi(i=1,2,..., N).;
Initialize the max numbers of iteration Tmax;
while T <Tmax do for each iteration
   if T%G equals 0 then
        Rank the chickens fitness values and establish a
        hierarchal order in the swarm;
        Divide the swarm into different groups, and
        determine the relationship between the chicks
        and mother hens in a group;
   end
   foreach chicken Xi in the swarm do
        if Xi is a roster then
          Update Xi's location using Eq. (26);
        end
        if Xi is a hen then
          Update Xi's location using Eq. (28);
        end
        if Xi is a chick then
          Update Xi's location using Eq. (31);
        end
        Evaluate the new solution using equation 34;
        If the new solution is better than its previous
        one, update it;
   end
end
```

Fig. 2. The semi-code of CSO optimization algorithm

5. Simulation and Results

A microgrid usually encompasses a set of distributed generation resources, energy storage utility, and the loads which can be operated as an active distribution network in two modes of islanding or connected to the upstream grid. The development of the microgrids is a subcategory of smart grid concept. The microgrid and smart grid concepts have both almost the same prime goals which are reduction in energy production costs, improvement in reliability state, and mounting the security of the system. Some advantages such as the development of green clean energy technologies in the distribution level and use of DRPs in the microgrids depends highly on the smart grid infrastructure. As can be seen in Fig. 3, the considered microgrid in this study consists of three load types of residential, commercial, and industrial. The generation power provider consists of MTs, wind turbines, solar cells, and battery. The considered microgrid is supposed to be capable to exchange power with the upstream grid. The characteristics of the installed generation resources are expressed in Table 1 as follows:

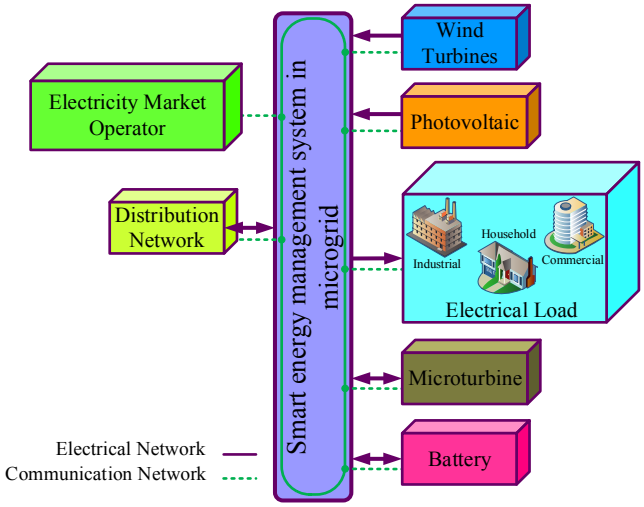

Fig. 3. The configuration of the considered microgrid

The designed location for implementation of the proposed grid-connected microgrid scheme is Sejzi town, which is located near the Isfahan city, Iran.

Table 1. The characteristics and emission factors relevant to the microgrid

Unit	NO_x (kg/MWh)	SO_2 (kg/MWh)	CO_2 (kg/MWh)	Offer ($\$/kWh$)	SUC & SDC ($\$$)	P_{max} (kW)	P_{min} (kW)
MT	0.23	0.0054	720	0.148	1.1227	200	30
WT	0	0	0	0.419	0	25	0
PV	0	0	0	1.017	0	50	0
Battery	0.001	0.0002	10	0.138	0	45	-45
Grid	2.1	0.5	950	-	0	500	-500

The town is about 35 km away from the center of Isfahan and in longitude ranges from 52°, 7′ *E*, the latitude ranges from 32° 42' *N*, and 1542 meters above the sea level. The plots of the Figs. 4 and 5 illustrate the power generated by wind turbines and photovoltaic cells as well as the total demand of the microgrid for each hour, respectively. The loads' types are residential, commercial and industrial. Hence the load curve of each type of consumption is depicted in Fig. 6 separately. The hourly price of electricity is considered as Fig. 7.

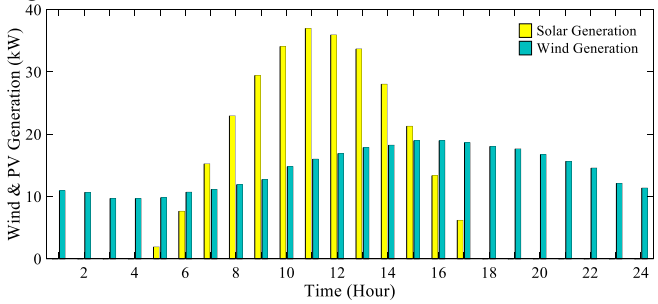

Fig. 4. The generation of the wind turbine and solar unit

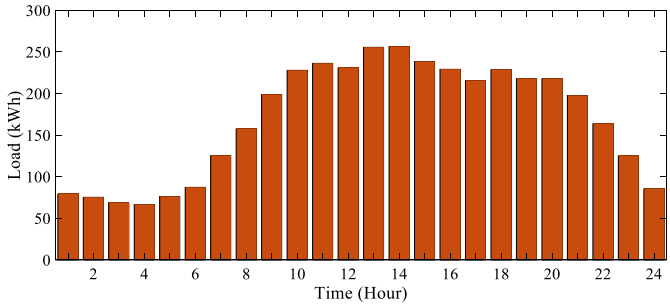

Fig. 5. The hourly load profile

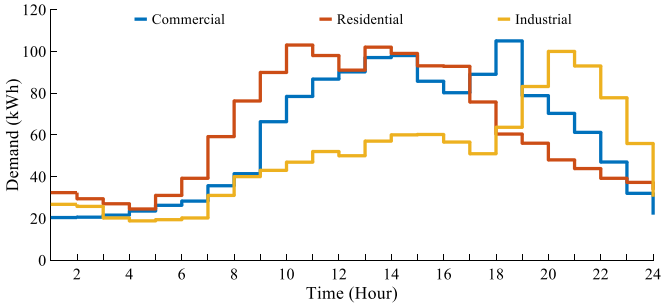

Fig. 6. The demand for various types of consumption

The purpose of this study is to maintain an optimized schedule with respect to the coordinated operation of microgrid's uncertain generation resources with energy storage facility. The objective of this scheme is to minimize the operational cost of the operation along with mitigation of emission.

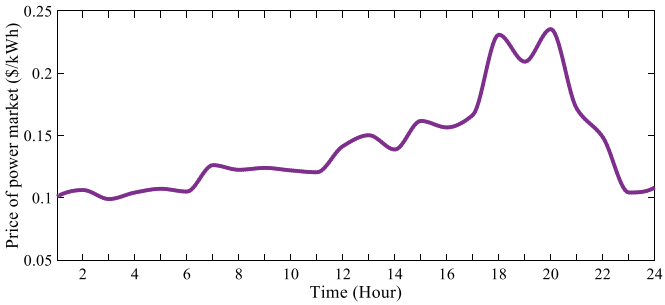

Fig. 7. The plot of the market clearing price

In addition, the impact of deployment of an incentive-based DRP is taken into account. In order to evaluate the effectiveness of the proposed scheme, three scenarios are defined as follows:

- Scenario 1: The microgrid is supplied completely from the upstream grid
- Scenario 2: The coordinated operation of distributed generation resources, storage units, and the grid subject to minimize operation and emission costs (Regardless of responsive loads)
- Scenario 3: The coordinated operation of distributed generation resources, storage units, and the grid subject to minimize operation and emission costs (with respect to the demand response resources)

5.1. Scenario 1

In this scenario, the whole demand of the microgrid is satisfied through the upstream grid. The total operation cost of the microgrid for a 24-hour period is obtained to be \$741.974. This cost comprised of \$611.470 due to purchasing electricity from the upstream grid and \$130.504 due to emission cost. The results show that the air contaminants of CO_2 by 3865.882 kg, SO_2 by 2.035 kg, and NO_x by 8.546 kg are produced over the timeframe of this study. Fig. 8 demonstrates the electricity price for the loads in scenario 1.

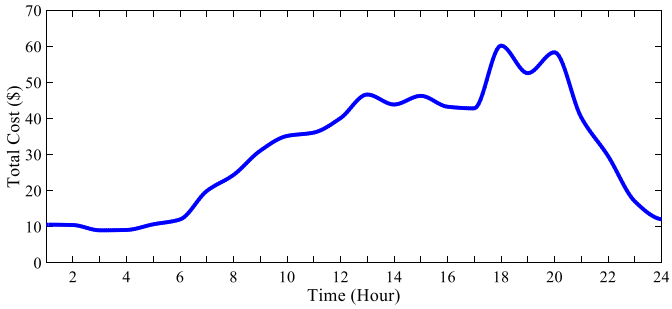

Fig. 8. The hourly price of electricity in scenario 1

5.2. Scenario 2

In the second scenario, the internal generation resources (as virtual power plants) and a storage unit are integrated into the operation model to meet the loads. Basically, in a restructured power system with a highly competitive and liquid environment, the system operator does not buy the excess generation of uncertain renewable resources and the surplus generation must be curtailed. However, in some restructured power systems with supporting policies for renewable generation, the trade criteria is a little different that facilitate more penetration of uncertain generation. After the emergence of microgrids and the advent of interconnected active distribution networks, it is suggested to dedicate some supporting policies for small-scale demand-side VPPs. Thus, in this study, the presumption is that the renewable resources can deliver their excess generated power to the main grid when the price of renewable generation is lower than the grid' price. In order to support renewable energy sources, the grid price will be paid to them when their bids are lower than the grid's price. On the contrary, when the price of electricity of microsources is higher than grid's price, the excess generation must be dedicated to the internal loads of the microgrid and the MT must balance the surplus generation and demand. Various generation resources can exist in a microgrid which requires proper scheduling in order to exploit more free green energy and avoid incurring unwanted costs. The commitment and dispatch schedule of microgrid resources are provided in Fig. 9. With respect to the objective function, the wind and solar units have the participation of 343.91 kW and 286.85 kW. Hence, the wind and solar unit earn $69.81 and $115.31 revenue from the sale of energy. The micro-turbine has generated 2023.45 kW which implies the maximum commitment among the generating units. The amount of generation is comprised of 1718.63 kW for the satisfaction of microgrid's loads and 304.82 kW that is sold to the main grid at peak hours. Hence, the revenue of $299.47 can be achieved by MT unit. The revenue of $66.04 is obtained for the MT unit from sell of energy to the main grid. The upstream grid has played also a prominent role in the satisfaction of demand by providing 1720.01 kW of electrical power which creates the revenue of $207.16. Fig. 10 depicts the sold and purchased electricity from the grid in various hours of study. As can be noticed from Fig. 8, the price of electricity sold to the grid at peak hours is higher than grid's electricity price. But at the rest of hours, the price of sold power is lower than grid's price.

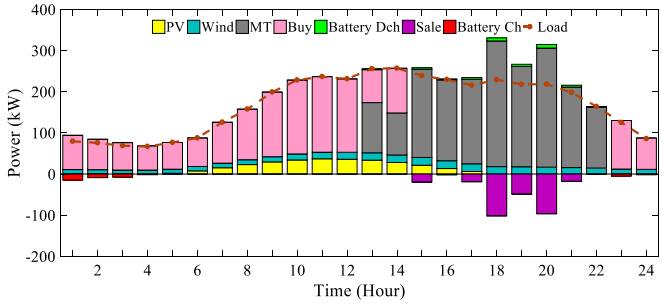

Fig. 9. The commitment and dispatch schedule of microgrid for distributed generation sources, storage unit, and grid (scenario 2)

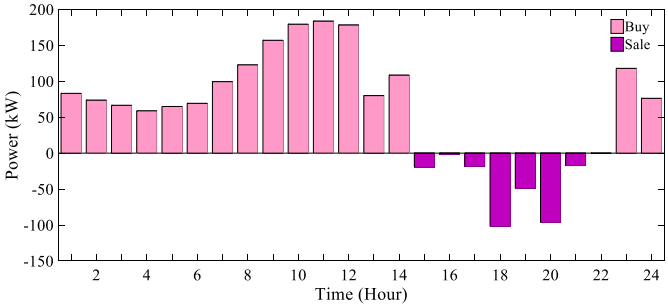

Fig. 10. The hourly sold and purchased power from the upstream grid (Scenario 2)

As can be seen in Fig. 10, the operator has decided to maintain the required energy of the microgrid by MT unit because the grid's price is higher than the generation price of MT, as figured out in Fig. 7. In addition, the excess capable generation of MT can be sold to the main grid, vice versa. The batteries function as storage units in the microgrid. Fig. 11 illustrates the time and amount of charge/discharge of batteries for operation schedule of batteries. As it is obvious, at the periods of 1-4 and 23-24, when the grid's electricity price is alleviated (compared with the selling price of batteries), the storage unit is planned to store 39.32 kW of power. At hours 13 and 15-22, when the price of electricity is increased in the grid, the operator of the microgrid has is inclined to discharge the batteries and to sell the stored electricity in the storage unit. During the entire time horizon, the battery has paid $4.04 to the grid for charging states and has earned the revenue of $5.43 from the sale of maximum capability of generation of stored energy. Thus, the Battery unit has profited by $1.38 over the course of this study.

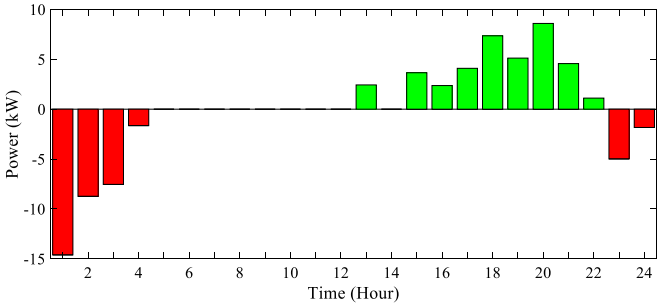

Fig. 11. The hourly charging and discharge schedule of battery unit (Scenario 2)

In this scenario, the total cost of demand provision is determined to be $714.56, which shows a reduction in comparison with the first scenario. The cost is composed of $627.09 corresponded with the generation cost of microsources and the costs of purchasing power from the main grid and $87.46 relevant to the detriments that must be paid due to emission. As can be noticed, due to the higher price of renewable resources (expected by the renewable owners because of higher capital costs) in comparison with grid's prices, the provision cost of demand by non-renewable resources is mounted in comparison with the first scenario. During hours 15-22, when the price of the grid is increased, the presence of wind, solar and MT units has resulted in mitigation of electricity price in comparison with supplying through the main grid. The presence of renewable and MT units has caused a significant emission reduction compared

with scenario 1 (2871 kg of CO_2, 0.869 kg of SO_2, and 4.007 kg of NO_x). The total cost of operation is decreased in comparison with the first scenario because of the role of renewable and MT units in emission reduction.

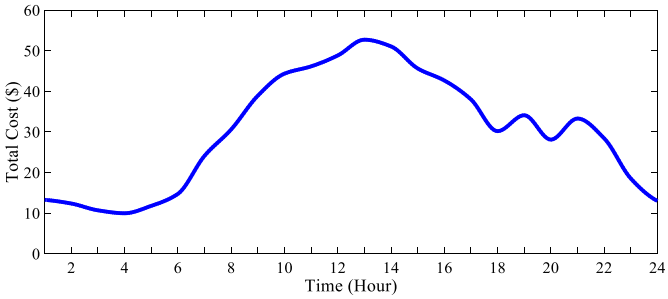

Fig. 12. The hourly price of electricity in scenario 2

5.3. Scenario 3

In this scenario, the scheduling is conducted while the implication of responsive loads is taken into account. The suggested voluntary packages for consumption reduction are in accordance with Table 2. The presumption of this study is that 40% of the total load would like to participate in the DRP. The execution of DRPs helps the operator to have more flexibility and maneuverability at peak hours. Fig. 13 depicts microgrid's load curve before and after the implementation of DRPs.

Table 2. The suggested DRP based on price per reduction

Off-peak	Reduction (kW)	0-10	10-20	20-100	100-140
	Price ($/kWh)	0.0102	0.0216	0.0289	0.0401
peak	Reduction (kW)	0-10	10-20	20-100	100-140
	Price ($/kWh)	0.0151	0.0325	0.0435	0.0657

By implementation of DRP in the 3rd scenario, the total consumption of the microgrid has mitigated from 4069.35 kW to 3380.35 kW. The commitment and dispatch schedule of generating units, storage unit, and power exchange with the main grid in alignment with scenario 3 is figured out in Fig 14. In this scenario, the micro-turbine unit has the participation of 2023.45 kW which shows a slight increase in generation. This amount is comprised of 1155.78 kW to satisfy internal loads of the microgrid and 907.61 kW that is sold to the main grid at peak. The former has provided the revenue of $171.05 and the latter has procured $187.62. These amounts indicate the total revenue of $358.67. It is clear that in the third scenario the MT unit is more inclined to sell energy to the grid as VPP. In the 3rd scenario, the bought power from the upstream grid is diminished to 1593.83 kW and the revenue of the grid from the source of sell of power to the microgrid is mitigated to $191.84. Fig. 15 demonstrates the amount of energy sold or bought to or from the main grid. As can be noticed from Figs. 14-16, the tendency of consumers to participate in DRP is increased within the interval of 15-20 (particularly, within 18-20).

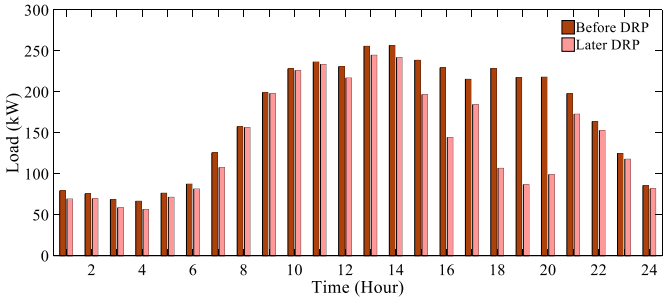

Fig. 13. The microgrid's load curve, before and after the execution of DRP

Hence, with respect to the DRP as well as the price discrepancies between instantaneous grid's prices and MT's Prices between 15 and 20, the microgrid's operator has tried to dedicate the maximum capacity of MT to sell energy to the main grid. Thus, the revenue and profit of MT unit are mounted compared with the 2nd scenario. The battery storage has virtually the same performance as the 2nd scenario. However, this unit has gained more profit because the batteries were able to sell more power to the main grid at peaks.

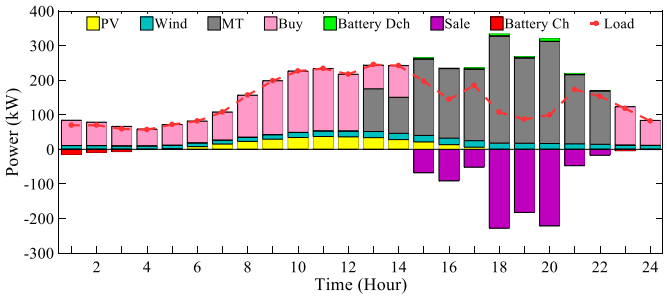

Fig. 14. The commitment and dispatch schedule of microgrid for distributed generation sources, storage unit, and grid (scenario 3)

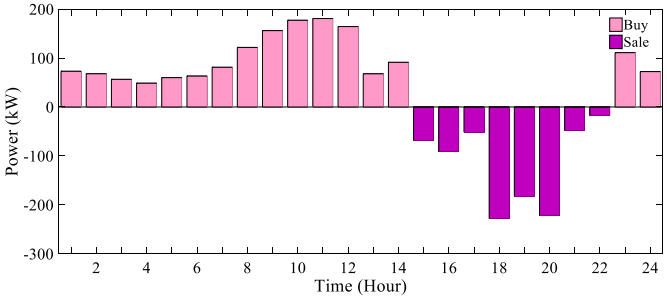

Fig. 15. The hourly sold and purchased power from the upstream grid (Scenario 3)

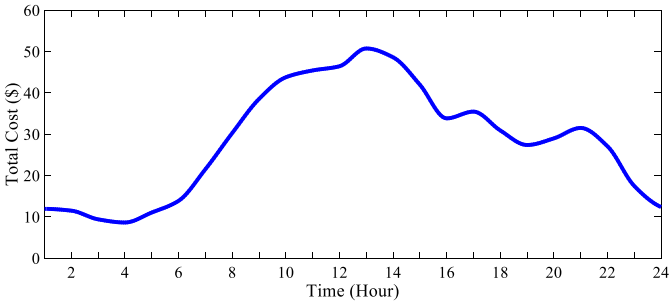

Fig. 16. The hourly cost of demand provision in scenario 3

In this respect, the battery unit has paid $4.06 for buying power from the grid and has received the revenue of $7.79 for selling the stored power to the grid which implies the profit of $3.73 over the course of study. In this scenario, the total operation cost of the microgrid within the timeframe of study is estimated to be $672.78, which constituted of $586.32 for the satisfaction of the microgrid's loads and $86.46 for the cost pertaining to emission detriment. The operation cost of the microgrid is correlated with the cost of buy of power from wind, solar, MT, battery, and upstream grid along with the cost of incentives that must be paid of DRP participants. According to Fig. 16, the final hourly cost of electricity for consumers based on scenario 3, which is composed of operation cost and emission cost, is alleviated compared with the previous two scenarios.

6. Conclusion

This study delves into the operation of a grid-connected microgrid comprised of wind, solar, micro-turbine generating resources which are also called microsources or virtual power plants (VPPs). Besides, the battery unit is utilized to redress the imbalances caused by renewable microsources. In addition, the impact of integration of demand response resources was also incorporated in the model. The purpose was to arrange an operation schedule for VPPs as a multi-objective problem subject to minimize the operation cost of the microgrid and emission cost. In addition, the profitability of the microgrid scheme is investigated based on hourly prices of the main grid and the possible power exchange with the upstream network. The model is assessed through three scenarios, and the results imply that the operation cost of the microgrid and emission cost can be effectively alleviated when the storage unit collaborates with uncertain microsources in the dispatch schedule and demand response capacities are enabled at peaks.

References

[1] Baghaee, H. R., Mirsalim, M., & Gharehpetian, G. B. "Multi-objective optimal power management and sizing of a reliable wind/PV microgrid with hydrogen energy storage using MOPSO." Journal of Intelligent & Fuzzy Systems 32, no. 3 (2017): 1753-1773.

[2] Sakurama, K., & Miura, M. "Communication-based decentralized demand response for smart microgrids." IEEE Transactions on Industrial Electronics 64, no. 6 (2017): 5192-5202.

[3] Javidsharifi, M., Niknam, T., Aghaei, J., & Mokryani, G. "Multi-objective short-term scheduling of a renewable-based microgrid in the presence of tidal resources and storage devices." Applied Energy 216 (2018): 367-381.

[4] Hosseini, S. J. A. D., Moradian, M., Shahinzadeh, H., & Ahmadi, S. "Optimal Placement of Distributed Generators with Regard to Reliability Assessment using Virus Colony Search Algorithm." International Journal of Renewable Energy Research (IJRER)8, no. 2 (2018): 714-723.

[5] Dufo-Lopez, R., Cristobal-Monreal, I. R., & Yusta, J. M. "Stochastic-heuristic methodology for the optimisation of components and control variables of PV-wind-diesel-battery stand-alone systems." Renewable Energy 99 (2016): 919-935.

[6] Scalfati, A., Iannuzzi, D., Fantauzzi, M., & Roscia, M. "Optimal sizing of distributed energy resources in smart microgrids: A mixed integer linear programming formulation." In Renewable Energy Research and Applications (ICRERA), 2017 IEEE 6th International Conference on, pp. 568-573. IEEE, 2017.

[7] Merabet, A., Ahmed, K. T., Ibrahim, H., Beguenane, R., & Ghias, A. M. "Energy management and control system for laboratory scale microgrid based wind-PV-battery." IEEE transactions on sustainable energy 8, no. 1 (2017): 145-154.

[8] Ross, M., Abbey, C., Bouffard, F., & Jos, G. "Multiobjective optimization dispatch for microgrids with a high penetration of renewable generation." IEEE Transactions on Sustainable Energy 6, no. 4 (2015): 1306-1314.

[9] Amrollahi, M. H., & Bathaee, S. M. T. "Techno-economic optimization of hybrid photovoltaic/wind generation together with energy storage system in a stand-alone micro-grid subjected to demand response." Applied Energy 202 (2017): 66-77.

[10] Parhizi, S., Khodaei, A., & Shahidehpour, M. "Market-Based Versus Price-Based Microgrid Optimal Scheduling." IEEE Transactions on Smart Grid 9, no. 2 (2018): 615-623.

[11] Farzin, H., Fotuhi-Firuzabad, M., & Moeini-Aghtaie, M. "A stochastic multi-objective framework for optimal scheduling of energy storage systems in microgrids." IEEE Transactions on Smart Grid 8, no. 1 (2017): 117-127.

[12] Tu, T., Rajarathnam, G. P., & Vassallo, A. M. "Optimization of a stand-alone photovoltaic–wind–diesel–battery system with multi-layered demand scheduling." Renewable energy 131 (2019): 333-347.

[13] Hytowitz, R. B., & Hedman, K. W. "Managing solar uncertainty in microgrid systems with stochastic unit commitment." Electric Power Systems Research 119 (2015): 111-118.

[14] Lv, T., Ai, Q., & Zhao, Y. "A bi-level multi-objective optimal operation of grid-connected microgrids." Electric Power Systems Research 131 (2016): 60-70.

[15] Farzin, H., Fotuhi-Firuzabad, M., & Moeini-Aghtaie, M. "Developing a stochastic approach for optimal scheduling of isolated microgrids." In Electrical Engineering (ICEE), 2015 23rd Iranian Conference on, pp. 1671-1676. IEEE, 2015.

[16] Kavousi-Fard, A., Niknam, T., & Fotuhi-Firuzabad, M. "Stochastic reconfiguration and optimal coordination of V2G plug-in electric vehicles considering correlated wind power generation." IEEE Transactions on Sustainable Energy 6, no. 3 (2015): 822-830.

[17] Baghaee, H. R., Mirsalim, M., Gharehpetian, G. B., & Talebi, H. A. "Reliability/cost-based multi-objective Pareto optimal design of stand-alone wind/PV/FC

generation microgrid system." Energy 115 (2016): 1022-1041.

[18] Hossain, E., Perez, R., & Bayindir, R. "Implementation of hybrid energy storage systems to compensate microgrid instability in the presence of constant power loads." In Renewable Energy Research and Applications (ICRERA), 2016 IEEE International Conference on, pp. 1068-1073. IEEE, 2016.

[19] Shaneh, M., Shahinzadeh, H., Moazzami, M., & Gharehpetian, G. B. "Optimal Sizing and Management of Hybrid Renewable Energy System for Highways Lighting." International Journal of Renewable Energy Research (IJRER)8, no. 4 (2018): 2336-2349.

[20] Moazzami, M., Hosseini, S. J. A. D., Shahinzadeh, H., Gharehpetian, G. B., & Moradi, J. "SCUC Considering Loads and Wind Power Forecasting Uncertainties Using Binary Gray Wolf Optimization Method." Majlesi Journal of Electrical Engineering 12, no. 4 (2018): 15-24.

[21] Moazzami, M., Ghanbari, M., Moradi, J., Shahinzadeh, H., & Gharehpetian, G. B. "Probabilistic SCUC Considering Implication of Compressed Air Energy Storage on Redressing Intermittent Load and Stochastic Wind Generation." International Journal of Renewable Energy Research (IJRER) 8, no. 2 (2018): 767-783.

[22] Shahinzadeh, H., Gharehpetian, G. B., Moazzami, M., Moradi, J., & Hosseinian, S. H. "Unit commitment in smart grids with wind farms using virus colony search algorithm and considering adopted bidding strategy." In Smart Grid Conference (SGC), 2017, pp. 1-9. IEEE, 2017.

[23] Moazzami, M., Fadaei, D., Shahinzadeh, H., & Fathi, S. H. "Optimal sizing and technical analysis of rural electrification alternatives in Kerman province." In Smart Grid Conference (SGC), 2017, pp. 1-8. IEEE, 2017.

[24] Nafisi, H., Agah, S. M. M., Abyaneh, H. A., & Abedi, M. "Two-stage optimization method for energy loss minimization in microgrid based on smart power management scheme of PHEVs." IEEE Transactions on Smart Grid 7, no. 3 (2016): 1268-1276.

[25] Shahinzadeh, H., Moazzami, M., Abbasi, M., Masoudi, H., & Sheigani, V. "Smart design and management of hybrid energy structures for isolated systems using biogeography-based optimization algorithm." In Smart Grids Conference (SGC), 2016, pp. 1-7. IEEE, 2016.

[26] Aguilera-Gonzalez, A., Vechiu, I., Rodriguez, R. H. L., & Bacha, S. "MPC Energy Management System for A Grid-Connected Renewable Energy/Battery Hybrid Power Plant." In 2018 7th International Conference on Renewable Energy Research and Applications (ICRERA), pp. 738-743. IEEE, 2018.

[27] Tooryan, F., Collins, E. R., Ahmadi, A., & Rangarajan, S. S. "Distributed generators optimal sizing and placement in a microgrid using PSO." In Renewable Energy Research and Applications (ICRERA), 2017 IEEE 6th International Conference on, pp. 614-619. IEEE, 2017.

[28] Moradi, J., Shahinzadeh, H., Khandan, A., & Moazzami, M. "A profitability investigation into the collaborative operation of wind and underwater compressed air energy storage units in the spot market." Energy 141 (2017): 1779-1794.

[29] Moazzami, M., Moradi, J., Shahinzadeh, H., Gharehpetian, G. B., & Mogoei, H. "Optimal Economic Operation of Microgrids Integrating Wind Farms and Advanced Rail Energy Storage System." International Journal of Renewable Energy Research (IJRER) 8, no. 2 (2018): 1155-1164.

[30] Shahinzadeh, H., Gheiratmand, A., Moradi, J., & Fathi, S. H. "Simultaneous operation of near-to-sea and off-shore wind farms with ocean renewable energy storage." In Renewable Energy & Distributed Generation (ICREDG), 2016 Iranian Conference on, pp. 38-44. IEEE, 2016.

[31] Moradi, J., Shahinzadeh, H., & Khandan, A. "A Cooperative Dispatch Model for the Coordination of the Wind and Pumped-storage Generating Companies in the Day-ahead Electricity Market." International Journal of Renewable Energy Research (IJRER) 7, no. 4 (2017): 2057-2067.

[32] Arbabzadeh, M., Johnson, J. X., Keoleian, G. A., Rasmussen, P. G., & Thompson, L. T. "Twelve principles for green energy storage in grid applications." Environmental science & technology 50, no. 2 (2015): 1046-1055.

[33] Arbabzadeh, M., Johnson, J. X., & Keoleian, G. A."Parameters driving environmental performance of energy storage systems across grid applications." Journal of Energy Storage 12 (2017): 11-28.

[34] Saim, A., Houari, A., Guerrero, J. M., Djerioui, A., Ahmed, M. A., & Machmoum, M. "Modeling of complex resonances in islanded Microgrids." In 2018 7th International Conference on Renewable Energy Research and Applications (ICRERA), pp. 804-808. IEEE, 2018.

[35] Baghaee, H. R., Mirsalim, M., Gharehpetian, G. B., & Talebi, H. A. "Application of RBF neural networks and unscented transformation in probabilistic power-flow of microgrids including correlated wind/PV units and plug-in hybrid electric vehicles." Simulation Modelling Practice and Theory 72 (2017): 51-68.

[36] Hovanessian, A., Norouzi, M. A., & Gharehpetian, G. B. "Demand response of islanded residential critical loads considering PV generation uncertainty and storage capacity." In Smart Grid Conference (SGC), 2017, pp. 1-8. IEEE, 2017.

[37] Meng, X., Liu, Y., Gao, X., & Zhang, H. "A new bio-inspired algorithm: chicken swarm optimization." In International conference in swarm intelligence, pp. 86-94. Springer, Cham, 2014.

[38] Wu, D., Xu, S., & Kong, F. "Convergence analysis and improvement of the chicken swarm optimization algorithm." IEEE Access 4 (2016): 9400-9412.